JVA
ISSN 1129-7298

J Vasc Access 2015; 16 (4): 275-284
DOI: 10.5301/jva.5000358

ORIGINAL ARTICLE

Fibrin sheath formation and intimal thickening after catheter placement in dog model: role of hemodynamic wall shear stress

Li Hua Wang, Fang Wei, Lan Jia, Zhi Lu, Bo Wang, Hong Ye Dong, Hai Bo Yu, Gui Jiang Sun, Jie Yang, Bo Li, Jia Meng, Rui Ning Zhang, Xue Qing Bi, Hai Yan Chen, Ai Li Jiang

Department of Kidney Disease and Blood Purification, Institute of Urology & Key Laboratory of Tianjin, 2nd Hospital of Tianjin Medical University, Tianjin - PR China

ABSTRACT

Purpose: To investigate the role of wall shear stress in aspects of the formation of fibrin sheath and intimal thickening in a dog model.

Methods: Tunneled silicone 14.5-F catheters were inserted into the left internal jugular vein in eight dogs. The dogs were separated into two groups according to catheter indwelling time of 14 and 28 days. All dogs underwent extracorporeal circulation three times a week. Multidetector computed tomography venography (MDCTV) examination was used to examine the catheter tip thrombus. After the animals were sacrificed, histological and immunohistochemistry evaluations were performed to confirm specific cell populations. We used computer modeling to generate wall shear stress profiles for the blood flow through the catheter.

Results: Catheter-related sheaths were identified in all catheter specimens, but there was no fibrin sheath around the catheter tip. There were also differences in wall shear stress between the different venous wall sites. Differences in vein wall thickening at different sites have been found at both 14 days (intima to media (I/M) ratio S1 vs S2: $p = 0.01$, S3 vs S4: $p<0.01$) and 28 days (I/M ratio S1 vs S2: $p<0.01$, S3 vs S4: $p<0.05$).

Conclusions: After catheter placement, fibrin sheath formation partially covered the catheter. Meanwhile, focal areas of intimal thickening were also seen in the venous wall adjacent to the sites of high wall shear stress. These findings indicate an important role of wall shear stress profiles in fibrin sheath formation and intimal thickening.

Keywords: Computational fluid dynamics, Hemodialysis, Tunneled catheter, Wall shear stress

Introduction

The clinical performance of a tunneled cuffed catheter is crucial for adequate hemodialysis. Several studies pertaining to blood flow rates, recirculation and long-term dysfunction-free survival have been conducted, but not many of them have focused on the performance of the catheters. The palindrome catheter (PC), which is a new design of catheter with symmetric tips and biased ports, is increasingly being used in recent years. In a study in a swine model using the PC, minimal recirculation was observed while dialysis lines were reversed, compared with split-tip and other catheters (1). However, the PC has also exhibited problems of catheter dysfunction in terms of fibrin sheath formation and venous stenosis (2, 3).

Accepted: December 21, 2014

Published online: February 7, 2015

Corresponding author:
Ai Li Jiang
23rd, Pingjiang Road, Hexi District
Tianjin, PR China, 300211
aili_j@163.com

Two important findings on the topic of catheter-related fibrin sheaths have been reported in the literature, namely the sheaths' histopathology features and the microscopic development. It is well established that a fibrin sleeve can cause encasement of the catheter, which can interfere with catheter function and lead to ineffective hemodialysis (4-7). On the other hand, there is a debate regarding the nature and pathophysiology of the development of intimal thickening, which correlates with venous stenosis (8, 9).

Although the pathology of stenosis has been extensively discussed in many studies, the exact etiopathogenesis of the disease is not fully understood. We hypothesize that the key factor which influences whether a venous wall will undergo stenosis is the hemodynamic wall shear stress (WSS) that is generated when extracorporeal circulation occurs after a catheter is inserted. Until now, several studies of WSS and pattern of stenosis in arteriovenous fistula have been reported (10, 11), and additionally a study using extracorporeal circulation to test catheter recirculation has been documented (12), but this study contains little data on the relationship of hemodynamic WSS to the formation of fibrin sheath, as well as to the development of intimal hyperplasia of the venous wall. For this reason, we used extracorporeal circulation and

computer modeling techniques to generate a WSS profile for the blood flow through the catheter to evaluate its performance, and to examine the fibrin sheath formation and the development of intimal hyperplasia in the superior vena cava wall that are adjacent to the central venous catheters in dogs.

Methods

Experimental design

A total of eight dogs (initial weight 25 kg) were used. Animal handling and experiment conformed to standards set forth in The Guide for the Care and Use of Laboratory Animals (13). The study was approved by the institutional animal use committee of the 2nd Affiliated Hospital of Tianjin Medical University, PR China. The dogs were divided into two groups (four in each group) and sacrificed after a catheterization period of 14 to 28 days.

Preoperative procedures: anesthesia

The dogs were anesthetized with xylazine hydrochloride injection (1 mg/kg, intramuscularly), at least 30 minutes prior to the surgical procedure.

Surgical preparation

All surgeries were performed using aseptic surgical procedures. The hair was shaved from the ventral and left lateral sides of the neck to at least the lateral midline on both sides. After the dogs were transferred into the operating room, the surgical site was cleaned by applying povidone-iodine solution onto its surface, followed by an application of 70% isopropyl alcohol and draping for aseptic surgery.

Surgical procedure

Percutaneous access to the left internal jugular vein was performed with ultrasound guidance. Access was achieved with a 21-gauge needle that was exchanged for a 3-coaxial dilator over a 0.018-inch guide wire (Covidien, Mansfield, MA, USA). A 16-F peel-away introducer sheath was advanced into the left internal jugular vein over a stiff 0.35-inch guide wire. The catheter used in this study was the 14.5-F 19-cm PC (Covidien). After catheter placement, an X-ray was taken to determine the location of the tip of the catheter. When the tip of the catheter was between the sixth and seventh ribs, we surmised that the catheter was in the proximal end of the superior vena cava according to our knowledge of canine anatomy.

Extracorporeal circulation

The dogs underwent extracorporeal circulation, under aseptic conditions, three times a week in order to simulate the hemodynamic conditions during hemodialysis. In brief, dogs were anesthetized, and subsequently, after priming with saline, two dialysis tubes were connected to the catheter adapters separately, and a loaded heparin dose of 3,000 IU was given intravenously. Finally, the dogs underwent extracorporeal circulation for 30 min, by using a blood pump with a blood flow rate of 250 mL/min. A heparin lock was used at the end of procedure, to prevent thrombosis.

Multidetector computed tomography venography examination

The dogs underwent multidetector computed tomography venography (MDCTV) at the 14-day and 28-day time points. MDCTV was performed using a 64-detector CT scanner (GE, Light speed VCT, Atlanta, GA, USA) after intravenous injection of 70 to 80 mL of Iohexol (350 mg/mL; GE Healthcare AS) via the venous adapter of the catheter at 3 mL/sec by a dual-head power injector (Tennessee XD2003, Ulrich GmbH & Co. KG, Ulm, Germany). Scanning was triggered automatically with bolus tracking and the region of interest was placed between the left internal jugular venous system and the superior vena cava, with a threshold of 100 Hounsfield units (HU), and a 5-sec fixed delay was used for data acquisition. The raw data were sent to an offline workstation (GE, Volume Share2-AW4.4 version), and then inputted into a three-dimensional software (GE, Volume Share2-AW4.4 version) on the workstation. Reconstruction images of the left internal jugular venous system and the superior vena cava were built by using multiplanar reformation, maximum intensity projection and volume rendering technique.

Specimen processing

The dogs were sacrificed after a catheterization period of 14 to 28 days. The tissues of the left internal jugular vein were fixed in formalin for at least 1 day. The tissue specimens were serially cut into five blocks, and numbered as sites1-5. Site 1 (S1) represented the area located 2 cm from the tip of the catheter; site 2 (S2) represented the area from the tip to the side holes of the catheter; site 3 (S3) represented the area around the side holes of the catheter; site 4 (S4) represented the area 2 cm from the side holes and site 5 (S5) represented the site of catheter entry (Fig. 1). Transverse slices of the associated venous wall of approximately 0.5 cm thickness were put into cassettes and embedded in paraffin.

Histochemistry and immunohistochemistry

Hematoxylin and eosin (H&E) staining was used for histological examination in the standard way. Verhoeff-van Gieson staining was used to identify elastic laminas and Masson's trichrome staining was used to visualize the collagen distribution. For the immunohistochemical staining, after deparaffinization and hydration, sections underwent antigen retrieval, were incubated with the blocking agent, 3% H_2O_2, for 10 min and blocked with rabbit serum for 30 min. The sections were then incubated with the primary antibody (anti-alpha smooth muscle actin antibody, abcam, ab5694, 1:100; and anti-von Willebrand factor abcam, ab6994, 1:200) overnight at 4°C. The next day, sections were incubated with the biotinylated goat anti-polyvalent antibody for 30 min and with streptavidin peroxidase for 30 min at 37°C. The sections were then treated with the DAB color developing

Fig. 1 - Photograph of internal jugular vein with an inserted catheter, divided into segments termed as segments 1-5: segment 1 (S1) represents the site located 2 cm from the tip of the catheter; segment 2 (S2) represents the area from the tip to the side holes of the catheter; segment 3 (S3) represents the area around the side holes of the catheter; segment 4 (S4) represents the site 2 cm from the side holes; segment 5 (S5) represents the site of catheter entry, after 28 days indwelling.

solution and hematoxylin. Following dehydration, sections were mounted and dried.

Development of a complete WSS profile

The computational domain encompasses the space in the blood vessel and the hemodialysis catheter which is being filled with blood. The computational domain was represented using a fine unstructured mesh of a number of tetrahedrons (ICEMCFD; version 14.5). In order to drive the flow in the computational domain, pressure boundary condition was set at both the inlet and the outlet ends of the blood vessel, and the flow boundary condition was set at both ends of the hemodialysis catheter. Due to the viscosity of blood, it is critically important in this study that nonslip boundary conditions are set at both the blood vessel wall and the hemodialysis catheter wall. The governing equation, that is, Navier-Stokes equation, which was discretized using the finite volume method and solved numerically (Fluent; version 14.5), resulted in the development of a complete calculated WSS distribution of the blood vessel inserted with a hemodialysis catheter (Fluent; version 6.3.26).

Image analysis

Images of the stained sections were digitalized using a microscope (Nikon Eclipse 90i) fitted with a camera head (DS-5M) and a controller (DS Camera Control Unit DS-L1), which delivered the image to a computer (IBM). Digital Managing System (NIS-Elements F.3.0) was used for image capture and analysis.

To calculate the thickness and area of the intimal and medial layers, the image analysis software was calibrated to report measurements in micrometer. For the H&E-stained sections, each segment was analyzed by drawing six equally spaced lines perpendicular to the venous wall and measuring the thickness of the intima and media. The data were then averaged to provide the thickness of the laminae for each segment and similar method was used for measuring the area of the intima and media.

Statistical analysis

The intima to media (I/M) ratios of both thickness and area from day 14 to day 28 were compared using Student's *t*-tests or alternatively Mann-Whitney *U* test when the data were not normally distributed. The difference was considered to be statistically significant at $p<0.05$. Statistical analysis was performed using the SPSS software version 20.0 (IBM Corporation, Armonk, NY, USA).

Results

Fibrin sheath formation and morphological changes of the venous vascular

At the histological examination, catheter-related sheaths partially covered the intravascular length of the catheter due to different catheter insertion period (Fig. 2). Whereas the fibrin sheath covered the catheter mainly from the entry site to the S4 site, there was no fibrin sheath around the catheter tip (S1-S3). The sheaths in the venous cavity were partially or circumferentially composed of a mixed cellular and noncellular coating of white blood cells embedded in thrombin (Fig. 3a, indicated by arrow) at day 14, while at day 28, there was less prominent cellularity and more prominent collagen content (Fig. 3b) in the fibrin sheaths. The intimal layer was located above the internal elastin layer (Fig. 4a, b). Additionally, smooth muscle cells were detected under the intimal layer at day 28, as indicated by their positive staining for the anti-actin antibody (Fig. 5a-d). Fibrin sheath formation was indentified at the site where the catheter was inserted into the left internal jugular vein, which we termed "S5." This finding was similar among all study groups at this site (Fig. 6a, b).

Results of MDCTV examination

At the 14-day time point, there was no obvious thrombus at the tip of the catheter (Fig. 7a), whereas at the 28-day time

Fig. 2 - Photograph of the internal jugular vein and well-developed, circumferential catheter-related sheath after 28 days indwelling time.

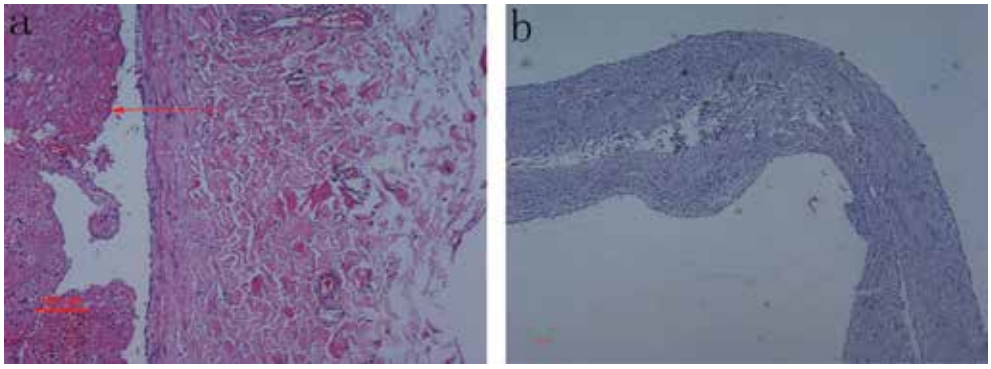

Fig. 3 - a) The sheaths in the venous cavity were partially or circumferentially composed of a mixed cellular and noncellular coating of white blood cells in a background of thrombin at day 14 (indicated by arrow) (H&E staining; original magnification, ×100). **b)** The sheaths in the venous cavity at day 28 showed less prominent cellularity and more prominent collagen content (H&E staining; original magnification, ×40).

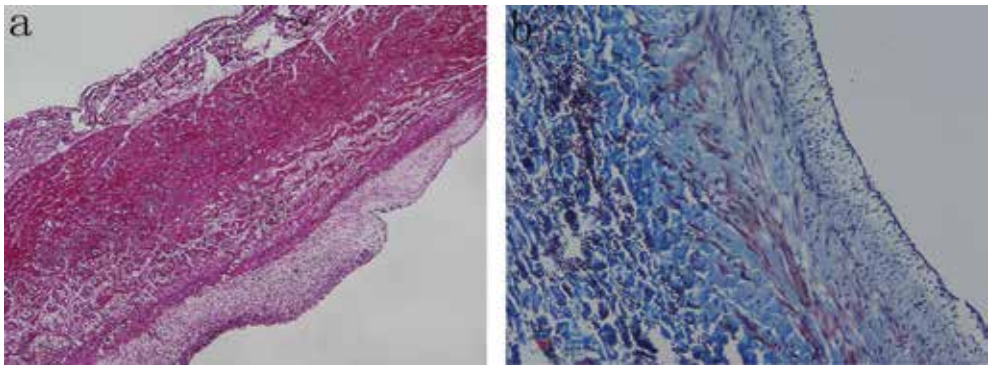

Fig. 4 - Collagen distribution in the laminar membrane was detected between intimal and media layers. **a)** Verhoeff-van Gieson's elastin (lamina) staining (original magnification, ×40). **b)** Masson's trichrome staining of collagen (original magnification, ×100).

point, there was thrombosis at the tip of the catheter (Fig. 7b, indicated by arrow).

Identification of differences of WSS values in S1-S4

We calculated the maximum and minimum WSS values as there was variation of WSS during extracorporeal circulation. The data show that the maximum WSS values were higher in S1 and S3, and lower in S2 and S4 (Fig. 8). Furthermore, the WSS value was highest on the S3 site compared to the other three sites. Figure 9a, b presents the WSS values calculated at the S3, S1 site during the peaks and valleys of blood flow circulation. The velocity vectors for both the cross-sectional and longitudinal sections have been analyzed in Figure 10a-c.

Identification of histological differences among S1-S4 sites with differences in WSS

At the 14-day time point, intimal hyperplasia could be found in the area located 2 cm from the tip of the catheter (S1), as well as the regions around the area of the side holes of the catheter (S3) (Fig. 11a, c). In contrast, Figure 11b and d

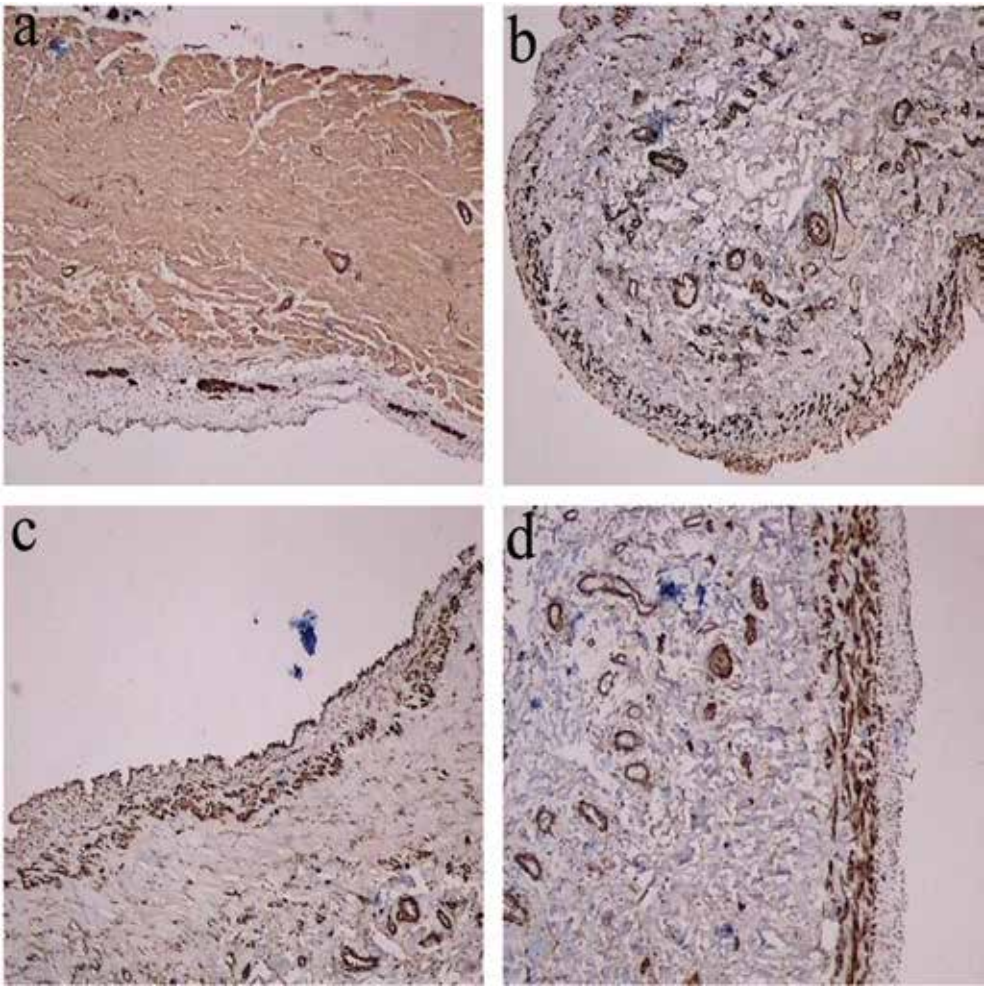

Fig. 5 - A 28-day specimen. Cells staining positive for smooth muscle actin were present under the intimal layer of the S1-S4 site. **a)** S1 site of the internal jugular vein. **b)** S2 site of internal jugular vein. **c)** S3 site of the internal jugular vein. **d)** S4 site of the internal jugular vein (H&E staining; original magnification, ×100).

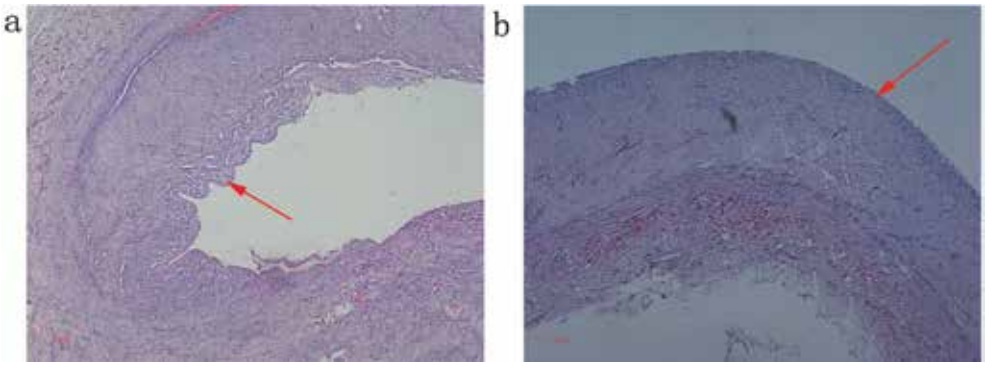

Fig. 6 - a) Fibrin sheath formation can be seen in the entry site in the internal jugular vein after 14 days indwelling time (arrow) (H&E staining; original magnification, ×40). **b)** Fibrin sheath formation can be seen in the entry site in the internal jugular vein after 28 days indwelling time (arrow) (H&E staining; original magnification, ×40).

shows that there was less intimal-media thickening in the S2 and S4 sites. Similar trend was observed for the 28-day time point on the S1-S4 sites (Fig. 12a-d). When the I/M ratio of the thickness was calculated, we found that the differences at the S1 and S2 sites ($p = 0.01$), as well as at the S3 and S4 sites, at 14 days ($p<0.01$), were statistically significant. Additionally, a similar trend was detected for the S1-S4 sites at the 28-day time point ($p<0.01$; $p<0.05$) (Figs. 13a, 14a). For I/M ratio of the area, we also observed a similar trend both at the 14-day time point (S1 vs S2: $p = 0.01$ S3 vs S4: $p<0.05$) and at the 28-day time point (S1 vs S2: $p<0.01$ S3 vs S4: $p<0.01$) (Figs. 13b, 14b). Furthermore, high maximum WSS values were detected in the S1 and S3 sites. These findings indicated that the greater differences in WSS between the S1 and S3 sites could correlate with the intimal-media thickening transition.

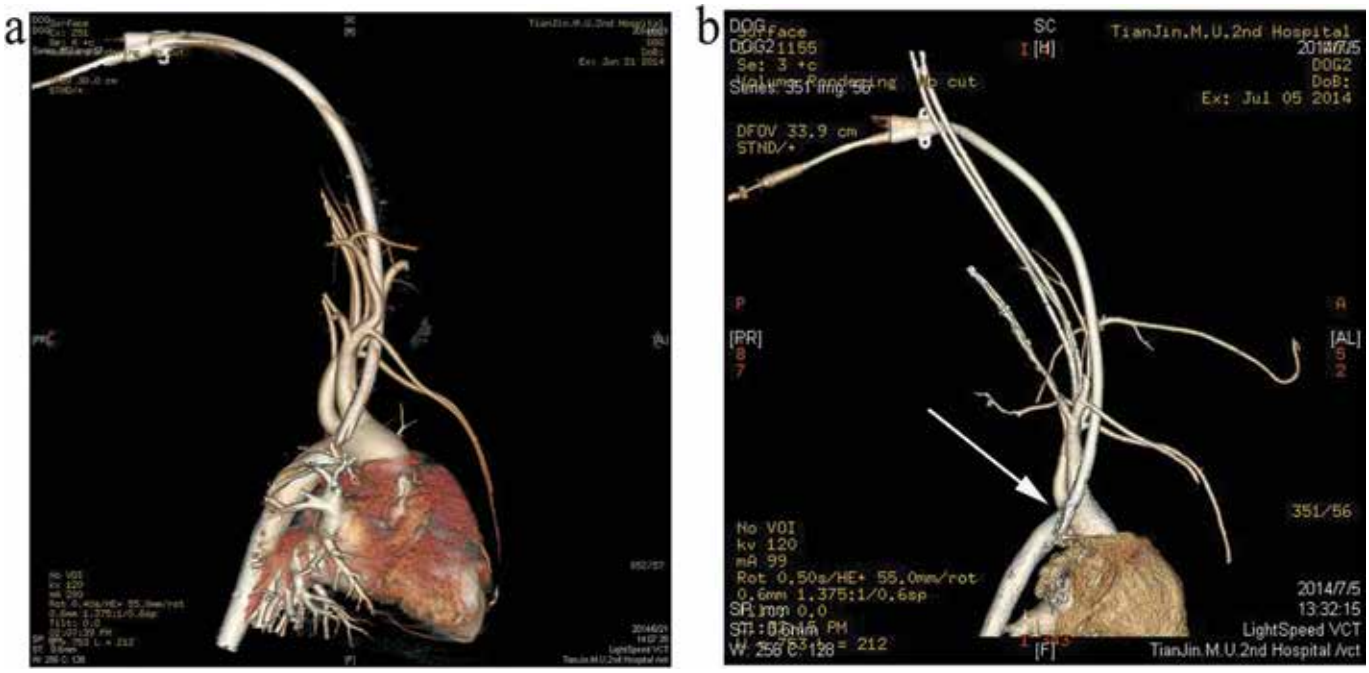

Fig. 7 - a) There was no obvious thrombus at the tip of the catheter at 14 days. **b)** There was thrombus at the tip of the catheter at 28 days (arrow).

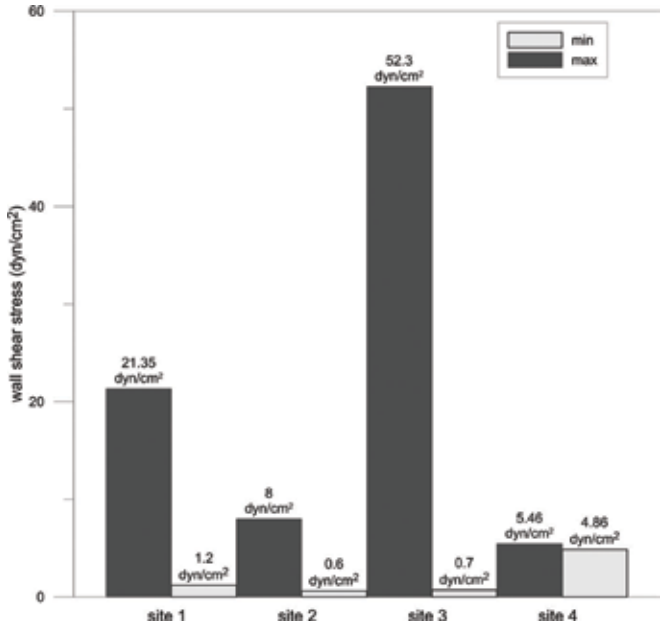

Fig. 8 - The maximum and minimum WSS values calculated during extracorporeal circulation. The maximum and minimum WSS values were high in the S1and S3 sites, and low in the S2 and S4 sites.

Discussion

The primary interests of this study were the development of the fibrin sheath and the histological changes of the adjacent vein while the dogs underwent extracorporeal circulation three times a week, which to our knowledge has not been previously reported. One of the main causes of catheter dysfunction is fibrin sheath formation, and it usually develops within 5-7 days after catheter placement (14-17). In this study, fibrin sheath formation was found in vascular wall at day 14, which is consistent with the findings of a frequently cited research (18) performed at autopsy in 55 patients with subclavian vein catheters.

Blood flow in the catheter results in WSS in the venous wall adjacent to the catheter. By using computational fluid dynamics (CFD), we found WSS differences in the S1-S4 sites and high maximum WSS values on the S1 and S3 sites, whereas there was no fibrin sheath formation on the S1-S3 sites. After examining the H&E staining, we found less intimal hyperplasia on the S2 and S4 sites, whereas intense intimal hyperplasia was observed on the S1 and S3 sites. Based on these findings, we hypothesized that WSS in the catheter during blood extracorporeal circulation may play an important role in regulating fibrin sheath formation and venous wall intimal hyperplasia. High WSS values may induce intimal hyperplasia and prevent the process of fibrin sheath formation during extracorporeal circulation.

Meanwhile, it has been suggested that catheter movement is another factor that causes intimal thickening. Catheter movement in the longitudinal direction has been demonstrated by several investigators (19-21). In addition, it has been found that respiratory movements and the heart beat in humans cause catheter floating in the blood flow and a knocking contact between the catheter and the vascular wall during radioscopy. Xiang et al hypothesized that in the larger diameter vein, the repeated microinjury caused by a catheter floating in the vessel lumen and knocking against a small area of the wall might result in the papillary form of intimal hyperplasia, while the repeated injury caused by the rubbing of the catheter against a broader area of the vein wall might result in plaque-like form of intimal hyperplasia (22). In this study, there was no morphological difference

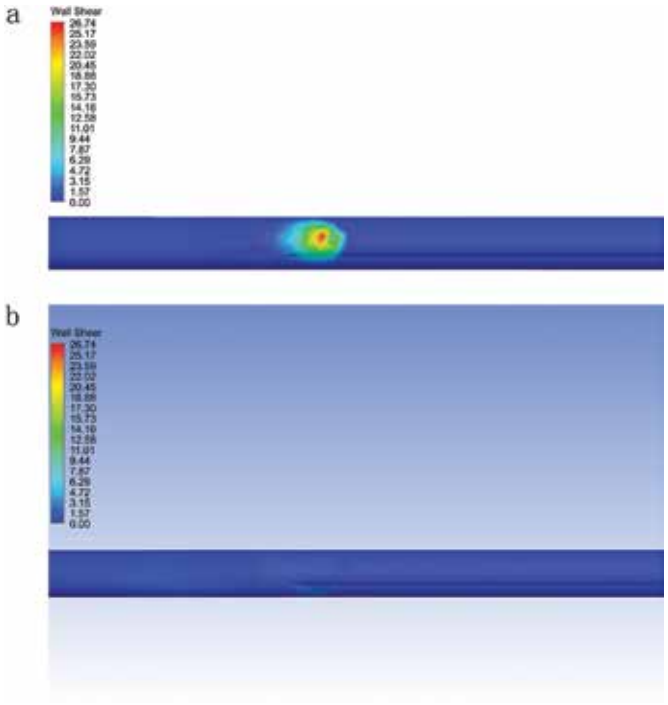

Fig. 9 - WSS contours of the catheter configuration during extracorporeal circulation. In this case, a hemodialysis catheter was inserted into a straight blood vessel at an angle of 20°. The length of the part of the hemodialysis catheter inserted in the blood vessel is 19 cm. The internal diameter and external diameter of the catheter are about 3.8 mm and 5 mm, and the internal diameter of the blood vessel is 1 cm. The three-dimensional computational domain was represented using a mesh of 1,997,302 tetrahedrons (ICEM CFD; version 14.5). In the hemodialysis catheter, the volume flow rate of blood was set to 250 mL/min. The pressure values at the inlet and the outlet boundaries of the blood vessel were set to 58.8 pa and 0 pa, respectively. Nonslip boundaries were set at both the blood vessel wall and the hemodialysis catheter wall. Addition of the flow data into this model, using finite volume method (Fluent; version 14.5), resulted in the development of a complete calculated WSS distribution of the blood vessel into which the hemodialysis catheter was inserted. Since the blood velocity at the hole of the venous end and the velocity gradient near the inner vascular wall are both large, the shear action on the inner vascular wall is larger near the catheter hole at the venous end. **a)** The WSS contours in the S3 section. **b)** The WSS contours in the S1 section.

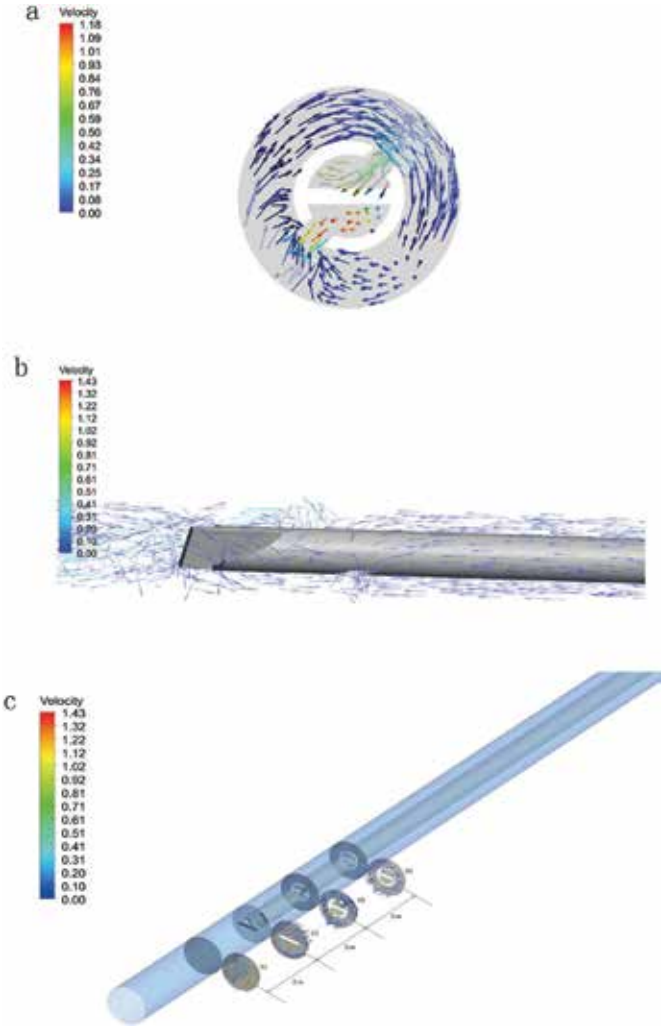

Fig. 10 - Velocity vectors for both the cross section and longitudinal level. Under the influence of the blood pressure drop, the blood flows away from the proximal end. The blood flows out of the catheter from the venous end and into the catheter from the arterial end. Because of the shear action of the blood, the flow is chaotic at the peripheral anterior of catheter. In addition, the blood velocity in this area is lower than that in the hole. **a)** The tangential component of the velocity vectors on the S3 cross section. **b)** The velocity vectors around the catheter. **c)** The tangential component of the velocity vectors on the S1-S4 cross section.

of the intimal hyperplasia. We theorized that the blood flow in the catheter also causes WSS to the adjacent vein wall during extracorporeal circulation, which is different from the condition in the Xiang et al study (22). Furthermore, the side holes in the S3 site may not be beneficial in extending catheter life when the catheter tip becomes occluded and blood flows through the side holes leading to vein intima damage and mural thrombus (23). Thus, suctioning from the side holes in combination with high WSS in this area may promote intimal thickening.

Studies have found the pericatheter thrombus infiltrated by numerous α-actin-positive cells which had migrated from the vein wall along adherent areas or connecting bridges in 7 days. This process transformed the thrombus into a pericatheter fibrin sleeve which mainly consisted of α-actin-positive cells and collagen (24, 25). Recently, Kohler and Kirkman reported that the thrombus at the catheter tip formed by infiltration of macrophages and smooth muscle cells (SMCs), resulting in a lesion similar to intimal hyperplasia (26). In our study, SMCs could be found under the intimal layer on the S1-S4 sites. But we did not find pericatheter fibrin around the catheter tip. This result again suggests that the process of fibrin sheath formation and intimal thickening may be influenced by the WSS of blood flow, the resulting dynamics and the subsequent response of the components of the venous wall to the catheter (27).

In this study, we found, by using MDCTV, that there was no thrombus at the catheter tip after 14 days, whereas there was thrombus at the catheter tip after 28 days. Thus, based on these results, we hypothesized that a pathologic process

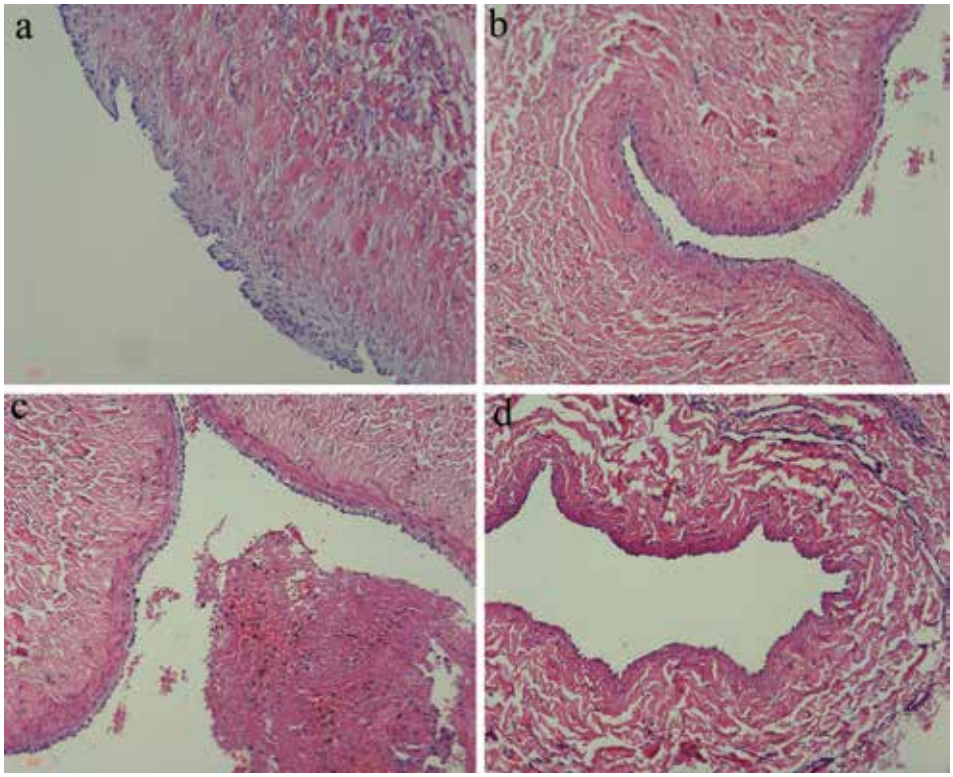

Fig. 11 - Intimal thickness of the S1-S4 site. **a)** Intimal thickness of the S1 site. **b)** Intimal thickness of the S2 site. **c)** Intimal thickness of the S3 site. **d)** Intimal thickness of the S4 site. 14-day specimen (H&E staining; original magnification, ×100).

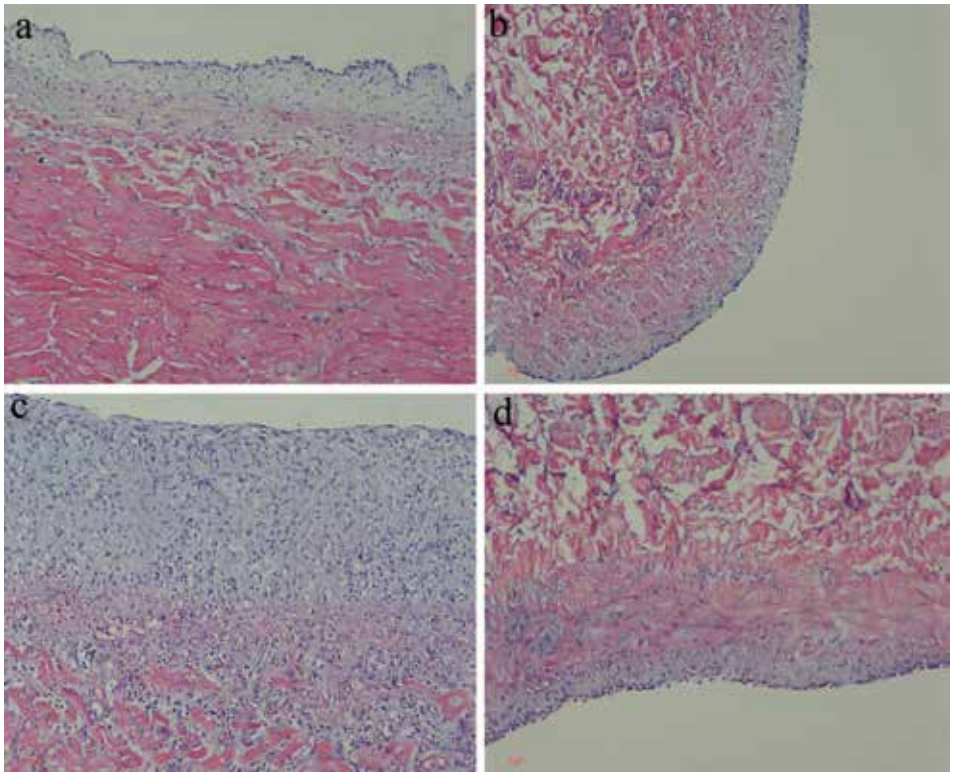

Fig. 12 - Intimal thickness of the S1-S4 site. **a)** Intimal thickness of the S1 site. **b)** Intimal thickness of the S2 site. **c)** Intimal thickness of the S3 site. **d)** Intimal thickness of the S4 site. 28-day specimen (H&E staining; original magnification, ×100).

may happen when thrombus forms adjacent to an indwelling catheter. This process is different from the common thrombus formation in vascular lumen, because the WSS generated after the catheter is inserted into the venous cavity may reduce thrombus formation during extracorporeal circulation (14, 28).

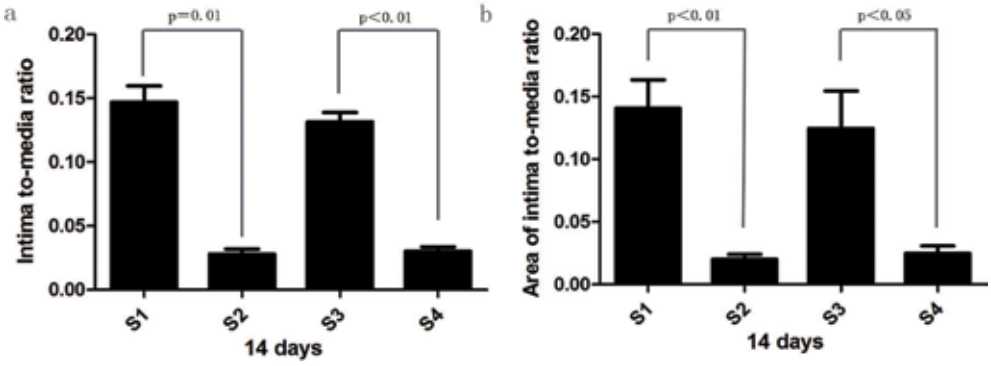

Fig. 13 - Intima to media ratio of both thickness and area in the S1-S4 site of 14 days. **a)** Thickness of intima to media ratio in the S1-S4 site after 14 days indwelling time. **b)** Area of intima to media ratio in the S1-S4 site after14 days indwelling time.

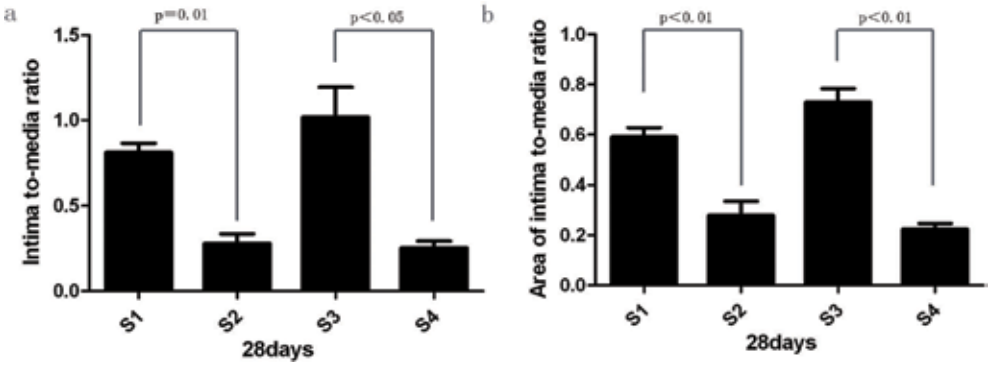

Fig. 14 - Intima to media ratio of both thickness and area in the S1-S4 site of 28 days. **a)** Thickness of intima to media ratio in the S1-S4 site after 28 days indwelling time. **b)** Area of intima to media ratio in the S1-S4 site after 28 days indwelling time.

The subsequent process of sheath formation is similar among animals and humans, but it is difficult to equate the results in a dog model with those found in humans (29, 30). Trauma due to catheter insertion, inherent properties of the catheter material or chronic rubbing of the catheter against the vein walls may be present singularly or in concert with one another. The response of the jugular and femoral vein wall to endothelial injury induced by trypsinization or air-drying has been studied in rabbit and rat models (31). In this dog model, the time course of the events cannot be extrapolated to human patients, but the common sequence of the response remains relatively constant and is consistent with previous studies in patients with short- and long-term indwelling catheters (18).

Our study has some limitations. Firstly, the number of dogs in each group was small. As reported in detail in another histological study (15) mainly about the catheter-related fibrin sheath, working with rodent models is easier to include a larger number of animals in the study, which is more difficult to do with canine models. But from our findings we have shown that there was difference of intimal thickening in different section of the vessel which was comparable with the difference of the WSS in the different sections developed from the CFD. Secondly, we did not measure the actual WSS inside the venous wall, which typically makes it difficult to apply these results to human studies. However, by using extracorporeal circulation, we simulate the hemodynamic condition during hemodialysis and consequently the sequence of events should be similar in terms of dynamics of the process and the ongoing response of the fibrin formation and intimal hyperplasia.

In conclusion, the fibrin sheath that forms around indwelling catheters in the dog model did not cover the whole catheter; meanwhile, focal areas of intimal thickening were also seen in the vein wall adjacent to the site of high maximum WSS values. The development is a dynamic process which involves WSS and not just the histological changes of non-cellular material and thrombus. We therefore believe that our findings could have clinical relevance, leading us to further study the relationship between hemodynamic profiles, molecular signaling and histological patterns.

Acknowledgments

The authors gratefully thank Professors Yuan and Li of Tianjin University for their help in creation of the CFD model. They also thank Dr Li for his help in the MDCTV examination. Li Hua Wang, Fang Wei and Lan Jia contributed equally to the work.

Disclosures

Financial support: None.
Conflict of interest: None.

References

1. Hwang HS, Kang SH, Choi SR, Sun IO, Park HS, Kim Y. Comparison of the palindrome vs. step-tip tunneled hemodialysis catheter: a prospective randomized trial. Semin Dial. 2012;25(5): 587-591.

2. Shanaah A, Brier M, Dwyer A. Fibrin sheath and its relation to subsequent events after tunneled dialysis catheter exchange. Semin Dial. 2013;26(6):733-737.
3. Agarwal AK. Central vein stenosis. Am J Kidney Dis. 2013;61(6): 1001-1015.
4. Kielstein JT, Kretschmer U, Ernst T, et al. Efficacy and cardiovascular tolerability of extended dialysis in critically ill patients: a randomized controlled study. Am J Kidney Dis. 2004;43(2): 342-349.
5. Oguzkurt L, Ozkan U, Torun D, Tercan F. Does a fibrin sheath formed around a catheter embolize upon removal of the catheter? Nephrol Dial Transplant. 2007;22(12):3677-3679.
6. Chan MR, Yevzlin AS. Tunneled dialysis catheters: recent trends and future directions. Adv Chronic Kidney Dis. 2009;16(5): 386-395.
7. Banerjee S. Dialysis catheters and their common complications: an update. Sci World J. 2009;9(9):1294-1299.
8. Osman OO, El-Magzoub AR, Elamin S. Prevalence and risk factors of central venous stenosis among prevalent hemodialysis patients, a single center experience. Arab J Nephrol Transplant. 2014;7(1):45-47.
9. Eleftheriadis T, Liakopoulos V, Antoniadi G, Pissas G, Leivaditis K, Stefanidis I. Late onset of clinically apparent central vein stenosis due to previous central venous catheter in a patient with inherited thrombophilia. Hemodial Int. 2014;18(2):540-543.
10. Krishnamoorthy MK, Banerjee RK, Wang Y, et al. Hemodynamic wall shear stress profiles influence the magnitude and pattern of stenosis in a pig AV fistula. Kidney Int. 2008;74(11): 1410-1419.
11. Haruguchi H, Teraoka S. Intimal hyperplasia and hemodynamic factors in arterial bypass and arteriovenous grafts: a review. J Artif Organs. 2003;6(4):227-235.
12. Tal MG. Comparison of recirculation percentage of the palindrome catheter and standard hemodialysis catheters in a swine model. J Vasc Interv Radiol. 2005;16(9):1237-1240.
13. NRC (National Research Council). The guide for the care and use of laboratory animals. Washington, DC: National Academy Press; 1996.
14. Vesely TM. Central venous catheter tip position: a continuing controversy. J Vasc Interv Radiol. 2003;14(5):527-534.
15. Beathard GA. Dysfunction of new catheters by old fibrin sheaths. Semin Dial. 2004;17(3):243-244.
16. Suhocki PV, Conlon PJ Jr, Knelson MH, Harland R, Schwab SJ. Silastic cuffed catheters for hemodialysis vascular access: thrombolytic and mechanical correction of malfunction. Am J Kidney Dis. 1996;28(3):379-386.
17. Rasmussen RL. The catheter-challenged patient and the need to recognize the recurrently dysfunctional tunneled dialysis catheter. Semin Dial. 2010;23(6):648-652.
18. Forauer AR, Theoharis C. Histologic changes in the human vein wall adjacent to indwelling central venous catheters. J Vasc Interv Radiol. 2003;14(9)(9 Pt 1):1163-1168.
19. Brandt RL, Foley WJ, Fink GH, Regan WJ. Mechanism of perforation of the heart with production of hydropericdium by a venous catheter and its prevention. Am J Surg. 1970;119(3):311-316.
20. Fischer GW, Scherz RG. Neck vein catheters and pericardial tamponade. Pediatrics. 1973;52(6):868-871.
21. Lingenfelter AL, Guskiewicz RA, Munson ES. Displacement of right atrial and endotracheal catheters with neck flexion. Anesth Analg. 1978;57(3):371-373.
22. Xiang DZ, Verbeken EK, Van Lommel AT, Stas M, De Wever I. Intimal hyperplasia after long-term venous catheterization. Eur Surg Res. 2000;32(4):236-245.
23. Moore HL. Side holes at the tip of chronic hemodialysis catheters are harmful. J Vasc Access. 2001;2(1):8-16.
24. Sugita C, Yamashita A, Moriguchi-Goto S, et al. Factor VIII contributes to platelet-fibrin thrombus formation via thrombin generation under low shear conditions. Thromb Res. 2009; 124(5):601-607.
25. Lucas TC, Tessarolo F, Veniero P, et al. Hemodialysis catheter thrombi: visualization and quantification of microstructures and cellular composition. J Vasc Access. 2013;14(3):257-263.
26. Kohler TR, Kirkman TR. Central venous catheter failure is induced by injury and can be prevented by stabilizing the catheter tip. J Vasc Surg. 1998;28(1):59-65, discussion 65-66.
27. Engstrom BI, Horvath JJ, Stewart JK, et al. Tunneled internal jugular hemodialysis catheters: impact of laterality and tip position on catheter dysfunction and infection rates. J Vasc Interv Radiol. 2013;24(9):1295-1302.
28. Forauer AR, Theoharis CG, Dasika NL. Jugular vein catheter placement: histologic features and development of catheter-related (fibrin) sheaths in a swine model. Radiology. 2006; 240(2):427-434.
29. Xiang DZ, Verbeken EK, Van Lommel ATL, Stas M, De Wever I. Composition and formation of the sleeve enveloping a central venous catheter. J Vasc Surg. 1998;28(2):260-271.
30. di Costanzo J, Sastre B, Choux R, Kasparian M. Mechanism of thrombogenesis during total parenteral nutrition: role of catheter composition. JPEN J Parenter Enteral Nutr. 1988;12(2): 190-194.
31. Manderson JA, Campbell GR. Venous response to endothelial denudation. Pathology. 1986;18(1):77-87.